An Evaluation of State-of-the-Art Projectors in the Presence of Noise and Nonlinearity in the Beer-Lambert Law

Shiyu Xie[1], Kai Zhang[1], and Alireza Entezari[1]

CISE Department, University of Florida, Gainesville, FL 32611-6120, USA
{shiyu.xie, zhangkai6}@ufl.edu, entezari@cise.ufl.edu

Abstract. Efficient computation of forward and back projection is key to scalability of iterative methods for low dose CT imaging at resolutions needed in clinical applications. State-of-the-art projectors provide computationally-efficient approximations to X-ray optics calculations in the forward model that strike a balance between speed and accuracy. While computational performance of these projectors are well studied, their accuracy is often analyzed in idealistic settings. When choosing a projector a key question is whether differences between projectors can impact image reconstruction in realistic settings where nonlinearity of the Beer-Lambert law and measurement noise may mask those differences. We present an approach for comparing the accuracy of projectors in practical settings where the effects of the Beer-Lambert law and measurement noise are captured by a sensitivity analysis of the forward model. Our experiments provide a comparative analysis of state-of-the-art projectors based on the impact of their approximations to the forward model on the reconstruction error. Our experiments suggest that the differences between projectors, measured by reconstruction errors, persists with noise in low-dose measurements and become significant in few-view imaging configurations.

Keywords: X-ray CT, forward model, fast projectors, iterative reconstruction

1 Introduction

X-ray imaging from low dose and/or limited views has a transformational value for CT imaging applications. Model-based iterative reconstruction (MBIR) algorithms integrate (statistical) models for X-ray optics, acquisition and image priors into an optimization framework for image reconstruction from limited X-ray data. One of the main challenges in using MBIR algorithms for imaging at resolutions relevant to clinical applications is their computational cost [3, 10, 4].

A key ingredient of MBIR algorithms is the forward model that provides a mathematical model for the acquisition process, following the Beer-Lambert law,

This project was supported in part by NSF grant CCF-2210866.

by relating the attenuation map, in the image domain, to the projection data, in the sinogram domain. For a particular imaging resolution, a linear approximation to the Beer-Lambert law is often used to construct a discretized forward model, $\boldsymbol{A}$, relating pixel/voxel intensities to detector measurements. The linear approximation of the Beer-Lambert law is widely adopted in the context of iterative reconstruction algorithms [2] and the artifacts (e.g., exponential edge gradient [7]) that arise from this approximation are well understood.

The computational challenges in iterative reconstruction algorithms stem from the fact that in practical resolutions the forward model is prohibitively large to be stored and reused during iterations. Instead, the forward projector $\boldsymbol{x} \mapsto \boldsymbol{A}\boldsymbol{x}$ and its adjoint, back-projector $\boldsymbol{y} \mapsto \boldsymbol{A}^T\boldsymbol{y}$, are computed on-the-fly during iterations. The computation of the forward model is the most expensive computation in MBIR algorithms.

Fast projectors reduce this computational burden, by introducing computationally efficient approximations to the integral transforms present in X-ray optics such as line integrals and detector blur calculations. Earlier methods for fast projection, such as pixel-driven, ray-driven [6] and distance-driven techniques use resampling techniques to reduce cost and state-of-the-art methods provide efficient approximations to the footprint of pixel/voxels in the detector domain (see section 3). Each of these methods strike a balance between the speed and accuracy for computation of the approximate forward model $\hat{\boldsymbol{A}}$. While the efficiency of fast projectors is assessed in terms of per-iteration computational cost, the accuracy of projectors not only impacts the quality of image reconstruction but also can impact the number of iterations necessary for convergence [13].

Contributions: Evaluation of fast projectors, from the accuracy perspective, in prior work is limited to idealistic settings where the quality of forward projection by $\hat{\boldsymbol{A}}$ from a discretized image is measured against the forward projection by a computationally-expensive reference projector $\boldsymbol{A}$ (e.g., [4, 9, 1]). When choosing a projection method, a key question is whether differences between accuracy of different projectors can impact image reconstruction in realistic settings where nonlinearity of the Beer-Lambert law and noise are present. This questions is nontrivial since the forward model, $\boldsymbol{A}$, is itself coming from a linearized approximation to the Beer-Lambert law and hence the differences among projectors could be insignificant in practical settings. We present an approach for comparing the accuracy of projectors in practical settings where effects of discretization errors, nonlinearity of the Beer-Lambert law and the Poisson noise in (low-dose) detector measurements are captured by a specialized notion of condition number based on the condition number of the forward model. We study the performance of state-of-the-art projectors in realistic settings on a phantom dataset where effects of the Beer-Lambert law is computable from exact line integrals in absence of discretization errors. Our study shows that the differences between projectors, measured by reconstruction errors, in realistic imaging conditions persist with measurement noise and the impact can only become less significant with large number of views.

2 Sensitivity Analysis of the Forward Model

Performance of algorithms on computational problems is generally characterized by sensitivity analysis of the problem with respect to perturbations of the input. In idealized settings the reconstruction problem can be formulated, algebraically, as a consistent system of equations, $\boldsymbol{Ax} = \boldsymbol{b}$ and iterative methods, such as SIRT, can be used for reconstruction and assessing accuracy of projectors (e.g., [4]). In this case, sensitivity analysis shows that the condition number of the forward model, $\text{cond}(\boldsymbol{A})$, determines the limits in the accuracy of the solution as well as the limits in performance of *any* iterative method for solving the system.

In practical CT reconstruction problems, effects of the Beer-Lambert law, noise in detector measurements as well as discretization errors lead to an inconsistent algebraic system whose conditioning not only depends on $\text{cond}(\boldsymbol{A})$ but also on the amount of inconsistency of the system. Given a discretization of the imaging domain, the forward model $\boldsymbol{A}$ calculates line-integrals over the image-space and integrates them over the detector cells. This computationally expensive projector is often used as reference projector [9, 4, 1, 13] and serves as the ideal forward model in the linearized approximation to the Beer-Lambert law. The vector of detector measurements $\boldsymbol{b}$ is obtained from line-integrals of the attenuation map whose exponential are integrated across detector cells capturing the nonlinearity of the Beer-Lambert law. The angle θ that the data $\boldsymbol{b}$ makes with (the span of) the column vectors of $\boldsymbol{A}$ provides a measure of inconsistency of the inverse problem and hence it depends on the strength of the Beer-Lambert law effect, magnitude of discretization errors, and the amount of noise in measurements. The sensitivity of the inconsistent problem depends not only on $\text{cond}(\boldsymbol{A})$ but also this angle θ.

Let $\hat{\boldsymbol{A}} = \boldsymbol{A} + \boldsymbol{\Delta A}$ denote the approximation introduced by a projector (Section 3). Moreover let $\boldsymbol{x} + \boldsymbol{\Delta x}$ be the solution to the perturbed inverse problem by the projector $\hat{\boldsymbol{A}}$. Then a first-order error analysis (e.g., [5]) shows: $\|\boldsymbol{\Delta x}\|/\|\boldsymbol{x}\| \leq \kappa \|\boldsymbol{\Delta A}\|/\|\boldsymbol{A}\|$ where the condition number is defined by:

$$\kappa := \left[(\text{cond}(\boldsymbol{A}))^2 \tan\theta + \text{cond}(\boldsymbol{A}) \right]. \tag{1}$$

In absence of the nonlinearity of the Beer-Lambert law (e.g., no detector blur) and discretization errors, $\boldsymbol{b}$ lies in the span of $\boldsymbol{A}$ (i.e., $\theta = 0$) and the sensitivity of the inverse problem reduces to $\text{cond}(\boldsymbol{A})$. However depending on the pixel and detector sizes the strength of the nonlinearity in the Beer-Lambert law increases $\theta > 0$ and the sensitivity of the problem becomes quadratically dependent on $\text{cond}(\boldsymbol{A})$. Moreover, the noise in measurements further impacts the condition as θ depends on the direction noisy measurements $\hat{\boldsymbol{b}}$ deviate from noiseless measurements $\boldsymbol{b}$ and the sensitivity of the problem needs to be analyzed statistically with an ensemble of noisy measurements. We study this condition number in fan beam geometry in section 4 that quantifies how the differences among fast projectors, in terms of accuracy, impacts image reconstruction accuracy.

3 Fast Projectors

Earlier approaches such as pixel-driven and ray-driven methods leverage interpolation/resampling techniques in image-domain and sinogram-domain for efficient forward and back projection operators. The distance-driven method resamples the image/sinogram signals from pixel and detector boundaries projected to a common plane according to the fan-beam geometry. State-of-the-art projectors provide a computationally efficient estimate of the contribution of a pixel to each detector that is used during forward and back projection.

Separable Footprints The SF [9] projector simplifies the line integration of pixel/voxel by approximating their footprints as trapezoidal/separable functions. This approximation allows for efficient calculation of their integral over detector cells. Compared to distance-driven methods, SF projectors are known to be more accurate and their computational cost are comparable in fan-beam and cone-beam geometries.

Look-up Table-based Ray Integration The LTRI [4] projector is an area-based method that computes the contribution of a pixel to a detector by the intersection area of source-detector triangle with that pixel. To reduce computations this method utilizes a pre-calculated look-up table, which is indexed by the perpendicular distance from the voxel center to the X-ray source-detector path, and the angle between the ray and a reference axis. The intersection area, which determines the weight of a voxel's contribution, is derived from the table using these parameters. GPU implementation of LTRI method is available and considered to be comparable in performance with the SF projector.

Non-Separable Footprints The CNSF projector [12, 13] derives the exact line integrals of pixel/voxels in the sinogram domain using an algebraic framework for directional convolution in the continuous domain. The integration over the detector cell is accomplished by back-projection of the detector cell on a central slice through the pixel/voxel resulting in a directional convolution in the image space. The line integrals of the directionally-blurred pixel are then computed exactly by piecewise polynomial functions that are efficiently evaluated during forward and back projection. This method eliminates the need for accessing memory that often limits the performance in GPU computations.

4 Experiment and Results

In this section, we first evaluate the sensitivity of the forward model under different (uniform) view counts for the least square solution to the inverse problem in presence of the nonlinearity of Beer-Lambert law as well as Poisson noise in detector measurements. This evaluation provides an upper bound for the impact (i.e., backward error) of the perturbation to the forward model introduced by fast projectors. Subsequently, we evaluate the root mean square error (RMSE) of

images reconstructed by SF, LTRI and CNSF projectors in comparison to the solution of the reference projector, under the Beer-Lambert law and varying noise levels. We utilized a field of view (FOV) of 100 mm × 100 mm. The simulation was conducted on a flat detector fan-beam CT system with a source-to-detector distance $D_{sd} = 156.25$ mm and a source-to-object distance $D_{so} = 78.125$ mm. To cover this FOV, each view has 855 detectors with each detector cell size of 0.78125 mm. As our goal is to quantify the differences in approximations present in these fast projectors at a large number of imaging configurations, we adopted a 128 × 128 resolution and employed a direct solver in sections 4.1, 4.2, and 4.3, eliminating the influence of finite iterations on the error analysis. In section 4.4, since the high resolution makes it impractical to use a direct solver, we employ the optimized gradient method [8] for fast projectors, aiming to compare the performance of projectors under low-dose conditions with practical iterative methods at a resolution of 256×256.

4.1 Sensitivity To Perturbations of the Forward Model

To assess the impact of using fast projectors, instead of computationally expensive reference projector, for solving the inverse problem, we establish the sensitivity of the inverse problem with respect to perturbations to the forward model. This actually reveals the upper bound of the backward error caused by the perturbations to fast projectors compared to the reference projector under different views. To that end, Fig. 1 shows this sensitivity, based on (1), as a function of the number of views. For this experiment the detector data $\boldsymbol{b}$ was calculated in presence of the Beer-Lambert law effects using numerical integration of line-integrals that are calculated analytically for the FORBILD dataset[11].

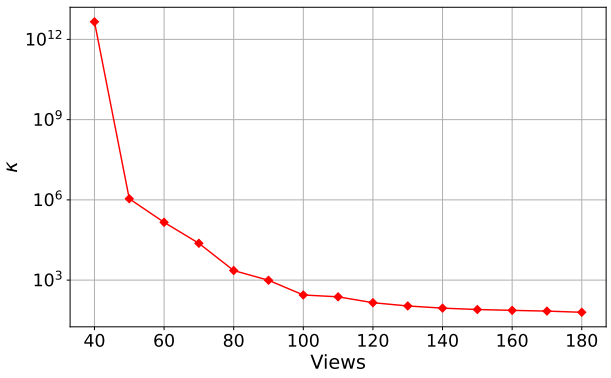

Fig. 1: Sensitivity of the inverse problem with respect to perturbations of the forward model.

As expected, for a large number of views, fast projector approximations to the forward model have little impact (i.e., proportional to $\|\boldsymbol{\Delta A}\|$) on the reconstruction as the condition number decreases. However with fewer number of views the impact of approximations brought about by fast projectors becomes more prominent as the condition number increases.

To assess the impact of noise on the sensitivity of the inverse problem, we also calculated an ensemble of noisy measurements according to a blank scan factor of $I_0 = 10^4$. Since the scale of perturbations at a small number of views is drastically different from that at a large number of views, many of the scatter plot points overlap. Therefore, we have expanded the scatter plot into a box plot, where the top and bottom numbers of the box plot represent the range of the scatter points. The length of the box plot is proportional to the logarithm of this range, so a longer box plot means the scatter points are more spread out, as shown in Fig. 2. This experiment illustrates the extent of variations introduced by noise in the sensitivity of the inverse problem with respect to perturbations introduced by fast projectors.

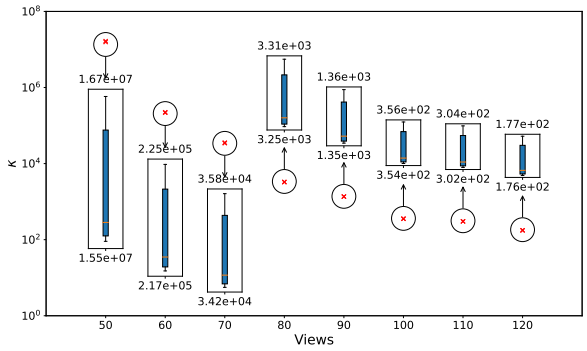

Fig. 2: Variations of the sensitivity measure under Poisson noise with blank scan factor of $I_0 = 10^4$.

4.2 Reconstruction Error

As the sensitivity analysis provides an upper bound on the impact of perturbations to the forward model on the solution, in this section we examine the actual perturbations introduced to the reconstructed images due to perturbations of the forward model by fast projectors. For this experiment the detector data $\boldsymbol{b}$ was calculated in presence of the Beer-Lambert law using numerical integration (on the detector cell) of line-integrals that are calculated analytically for the FORBILD dataset. Fig. 3 shows the RMSE in images reconstructed by

SF, LTRI and CNSF compared to the reconstruction provided by the reference projector at a given number of views.

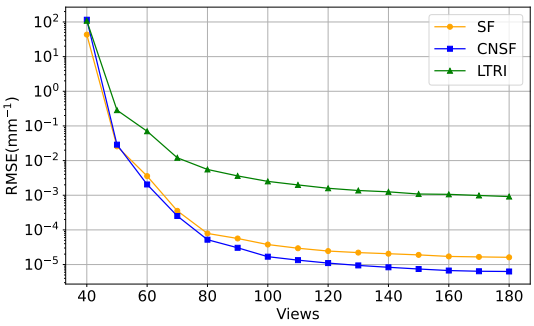

Fig. 3: The RMSE performance of fast projectors compared with the Ref projector at different number of views under the influence of the Beer-Lambert law and discretization error.

At 40 views, the SF projector has the lowest RMSE, showing the best performance. By 50 views, the RMSE of SF is very close to that of CNSF, indicating comparable image reconstruction accuracy. However, from 60 views onwards, CNSF surpasses SF with a consistently lower RMSE. The LTRI projector has the highest RMSE at all view counts, suggesting it has the lowest reconstruction accuracy. In our experiments, we also observed that the differences between projectors become negligible for a large number of views (i.e., 360 in this setting).

4.3 Reconstruction Error in Presence of Poisson Noise

To assess the impact of measurement noise on the differences between fast projectors, we collected an ensemble of noisy measurements $\hat{\boldsymbol{b}}$ by simulating a Poisson process [2] for detector counts at high noise setting.

Since the scale of variability in the error in image reconstruction, from noisy measurements, is highly different for a small versus large number of views, we visualized the variabilities in a scatter plot and expanded it into a box plot, where the length of the box plot is proportional to the inverse of the logarithm of the range, to show in Fig. 4.

4.4 Reconstruction Result

Fig. 5 shows the reconstruction result of the FORBILD head phantom with a field of view (FOV) of $100\,\text{mm} \times 100\,\text{mm}$, at the resolution of 256×256 by the reference projector (top left) and the differences in image reconstruction brought about by fast projectors. This experiment suggests that under the conditions of

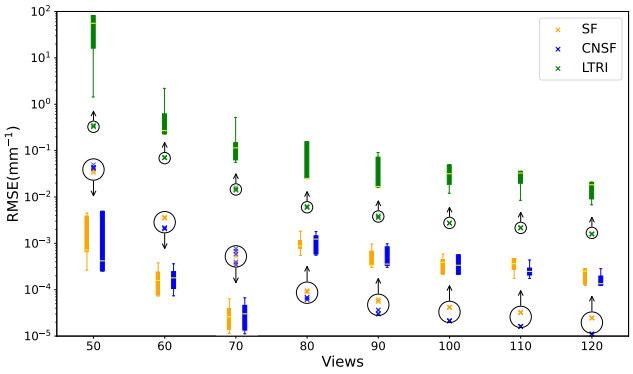

Fig. 4: The RMSE performance of fast projectors compared with the Ref projector at different number of views under the influence of the Beer-Lambert law, discretization error and high noise (blank scan factor 5×10^4).

high noise and the presence of the Beer-Lambert Law, the error reconstructed images follow the accuracy of projectors as CNSF is closer to the reference projector, followed by SF, and lastly LTRI.

5 Conclusion

Our analysis of the sensitivity of the inverse problem provides a basis for comparison of fast projectors and assessing the impact of their differences in image reconstruction. Our experiments suggest that area-based projectors compared to line-integral methods may have an inherently larger error in reconstructed images. For low-dose CT applications, the projectors with most accurate computation of line integrals provide the most robust imaging results. CNSF calculates the line integral exactly and approximates the detector blur, whereas SF approximates the line integral over the detector cell, leading to differences in the results. Furthermore, LTRI that approximates the line integrals across the detector by an area calculation, introduce more significant errors that are observable in reconstructed images. As the differences between projectors become less significant with large set of views, the accuracy of computing the forward model becomes important for few-view imaging applications. Moreover, the differences between projectors persist in presence of nonlinearity of the Beer-Lambert law and levels of Poisson noise in detector data. Future work includes evaluation of the role of (quadratic) regularization in sensitivity of the inverse problem and examination of these projectors in cone-beam geometry.

Code Availability. The code and data of this study has been made available at https://github.com/ShiyuXie0116/Evaluation-of-Projectors-Noise-Nonlinearity.

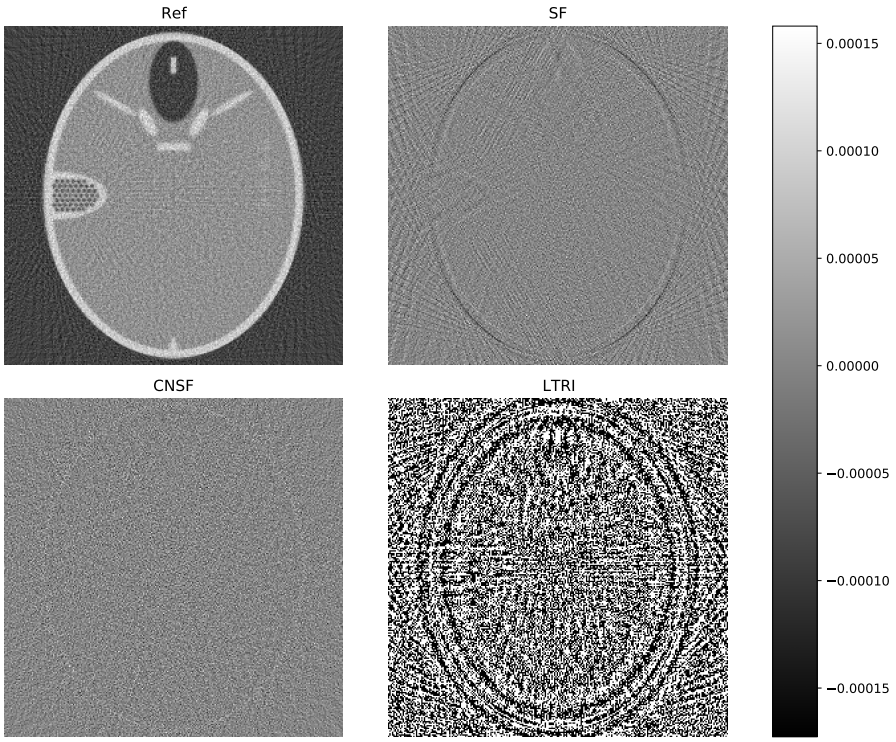

Fig. 5: Reconstruction of FORBILD head phantom from 90 uniformly spaced projections by Ref projector (top left), in presence of the nonlinearity in the Beer-Lambert law and high noise (blank scan factor of $I_0 = 5 \times 10^4$), using the optimized gradient method [8] with 50 iterations. The differences between fast projectors and Ref projector are shown in the other three images.

Disclosure of Interests. The authors have no competing interests to declare that are relevant to the content of this article.

References

1. De Man, B., Basu, S.: Distance-driven projection and backprojection. In: 2002 IEEE Nuclear Science Symposium Conference Record. vol. 3, pp. 1477–1480. IEEE (2002)
2. Fessler, J.A.: Statistical image reconstruction methods for transmission tomography. Handbook of medical imaging **2**, 1–70 (2000)
3. Geyer, L.L., Schoepf, U.J., Meinel, F.G., Nance Jr, J.W., Bastarrika, G., Leipsic, J.A., Paul, N.S., Rengo, M., Laghi, A., De Cecco, C.N.: State of the art: iterative CT reconstruction techniques. Radiology **276**(2), 339–357 (2015)
4. Ha, S., Mueller, K.: A look-up table-based ray integration framework for 2-d/3-d forward and back projection in X-ray CT. IEEE transactions on medical imaging **37**(2), 361–371 (2017)

5. Heath, M.T.: Scientific Computing: An Introductory Survey, Revised Second Edition, chap. 3, pp. 105–156. SIAM (2018)
6. Huesman, R., Gullberg, G., Greenberg, W., Budinger, T.: Users manual: Donner algorithms for reconstruction tomography (1977)
7. Joseph, P.M., Spital, R.: The exponential edge-gradient effect in X-ray computed tomography. Physics in Medicine & Biology **26**(3), 473 (1981)
8. Kim, D., Fessler, J.A.: On the convergence analysis of the optimized gradient method. Journal of optimization theory and applications **172**(1), 187–205 (2017)
9. Long, Y., Fessler, J.A., Balter, J.M.: 3d forward and back-projection for X-ray CT using separable footprints. IEEE transactions on medical imaging **29**(11), 1839–1850 (2010)
10. Willemink, M.J., Noël, P.B.: The evolution of image reconstruction for CT—from filtered back projection to artificial intelligence. European radiology **29**, 2185–2195 (2019)
11. Yu, Z., Noo, F., Dennerlein, F., Wunderlich, A., Lauritsch, G., Hornegger, J.: Simulation tools for two-dimensional experiments in X-ray computed tomography using the FORBILD head phantom. Physics in Medicine & Biology **57**(13), N237 (2012)
12. Zhang, K., Entezari, A.: A convolutional framework for forward and back-projection in fan-beam geometry. In: 2019 IEEE 16th International Symposium on Biomedical Imaging (ISBI 2019). pp. 1455–1458. IEEE (2019)
13. Zhang, K., Entezari, A.: Convolutional forward models for X-Ray computed tomography. SIAM Journal on Imaging Sciences **16**(4), 1953–1977 (2023)